Postselection of a polarization basis in intensity correlations under electromagnetically induced transparency

Hee Jung Lee, Taek Jeong, and Han Seb Moon*
Department of Physics, Pusan National University, Busan 609-735, Korea
(Received 7 June 2014; published 25 September 2014)

We report on switching the intensity correlation or anticorrelation by changing the polarization basis for measuring light that has already propagated through the electromagnetically induced transparency (EIT) medium of the $5S_{1/2}(F=2)-5P_{1/2}(F'=1)$ transition of ^{87}Rb atoms. When a linearly polarized laser beam interacts with the EIT medium in the Hanle configuration, selection of the polarization basis after the optical field has already interacted with the atoms was found to significantly affect the intensity-intensity correlation of the two orthogonal polarization components. We compared the second-order correlation functions of two postselected polarization bases (linear and circular), and the polarization basis effect on the second-order correlation functions as a function of the applied magnetic field was numerically calculated using an eight-level atomic model.

DOI: 10.1103/PhysRevA.90.033843 PACS number(s): 42.50.Gy, 32.80.Qk, 32.80.Wr

I. INTRODUCTION

The interaction between multilevel atoms and coherent optical fields is understood in terms of the quantum interference due to atomic coherence between atomic states [1]. Electromagnetically induced transparency (EIT) is a well-known representative phenomenon of two-photon coherence [1–6] and is useful in its ability to induce dramatic changes in the light properties, such as the intensity, phase, and group velocity, because of the narrow transparency window and steep dispersion that is created [6–10]. Recently, two-photon quantum coherence has been exploited in quantum optics applications, including quantum memory, quantum repeaters, squeezed photons, and paired-photon generation [11–21].

Two coherent optical fields that interact with a Λ-type atomic system composed of one common excited state and two ground states will be strongly correlated because of the quantum interference effect. Intensity correlations between two independent lasers have been experimentally demonstrated under EIT [22,23]. Scully and co-workers [24–26] have experimentally and theoretically studied the intensity fluctuations between orthogonal polarization components (generated by splitting a single laser beam, rotating the polarization of one resulting beam, and then recombining the beams) using an EIT medium with the Hanle configuration. The correlation and anticorrelation between the two optical fields have been interpreted as a conversion of the phase fluctuation between the two orthogonally polarized lasers into an amplitude fluctuation owing to the narrow transparency window and steep variation in the refractive index around the two-photon resonance condition [27].

There are two types of polarization basis sets composed of either (1) orthogonal linear polarization states or (2) counter-rotating circular polarization states. Previous studies of the intensity correlations in EIT determined the polarization basis of the incident laser before the atom-light interaction and then measured the intensity correlation between the two polarization basis components, as shown in Fig. 1. This means that the polarization of the incident laser beam needs to be prepared according to the desired intensity correlation, i.e., that between counter-rotating circularly or orthogonal linearly polarized components [24–26]. Therefore, as shown in Fig. 1, previous studies have demonstrated the intensity correlations of the circular and linear polarizations independently with an EIT medium [24–27].

In this study, the polarization of the incident laser beam was set to be linear, and we investigated the intensity-intensity correlation by selecting the orthogonal polarization basis after the beam had propagation through an EIT medium of the $5S_{1/2}(F=2)-5P_{1/2}(F'=1)$ transition of ^{87}Rb atoms. Under the same conditions for the interaction of the atoms with the coherent optical fields, we measured the intensity cross-correlation function between two orthogonal polarization components to investigate the change in the intensity correlation according to the selected polarization basis. In addition, the dependence of the second-order cross-correlation function on the incident power was investigated for counter-rotating circularly polarized components. Using an eight-level atomic system model, we numerically calculated the polarization basis effect in the correlation of the EIT as a function of the applied magnetic field.

II. EXPERIMENTAL SETUP

Figure 2 shows two energy-level diagrams of the magnetic sublevels of the $5S_{1/2}(F_g=2)\rightarrow 5P_{1/2}(F_e=1)$ transition of ^{87}Rb atoms based on the quantization axis; the energy levels are coupled by a laser beam that is linearly polarized at an angle of 45° with respect to the x axis. When the quantization axis and propagation direction of the laser are parallel to the z axis, there are $\sigma^+(\Delta m=+1)$ and $\sigma^-(\Delta m=-1)$ transitions between the magnetic sublevels [Fig. 2(a)] because the linearly polarized light may be considered as being composed of counter-rotating circularly polarized components. However, if the quantization axis is parallel to the x axis and the propagation of the laser is along the z axis, then $\pi(\Delta m=0)$ and $\sigma^{\pm}(\Delta m=\pm 1)$ transitions between the Zeeman sublevels are possible [Fig. 2(b)] owing to the two perpendicular linearly polarized components. As is well known, the measured intensity-intensity correlation after the atom-light interaction is independent of the quantization axis because the two

*Corresponding author: hsmoon@pusan.ac.kr

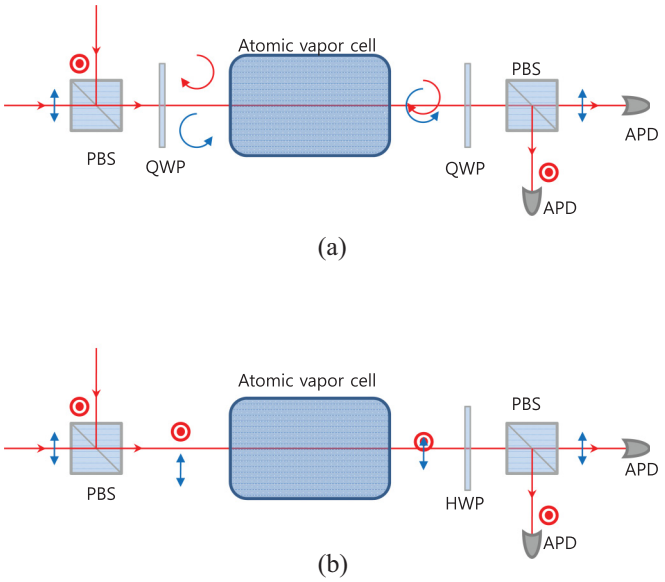

FIG. 1. (Color online) Schematics of the experimental setup for measuring the intensity correlation between (a) counter-rotating circularly polarized components and (b) orthogonal linearly polarized components. PBS: polarizer beam splitter, HWP: half-wave plate, QWP: quarter-wave plate, and APD: avalanche photodiode.

transitions among the Zeeman sublevels are related to an axis transformation. However, in considering the atom-light interaction in the presence of an external magnetic field, we selected the direction of the quantization axis to be that of the external magnetic field to simplify the calculation of the atomic transitions. Based on the polarization basis after the interaction with the EIT medium, we investigated how the intensity correlation between two counter-rotating circularly polarized components from the σ^+ ($\Delta m = +1$) and σ^- ($\Delta m = -1$) transitions differed from that between two perpendicular linearly polarized components.

In our experiment, the Hanle configuration was achieved by setting the longitudinal magnetic field B_l to be parallel to the propagation of the laser in the Rb atomic vapor cell. Figure 3 shows a schematic of our experimental setup. The laser beam passes through a 7-cm-long Rb vapor cell, which was surrounded by a solenoid coil, heating system, and μ-metal magnetic shield. This setup is similar to that used in

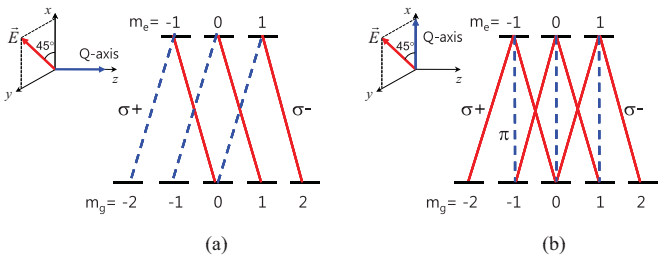

FIG. 2. (Color online) Two different energy-level diagrams of the magnetic sublevels of the $5S_{1/2}(F_g = 2) \rightarrow 5P_{1/2}(F_e = 1)$ transition of ^{87}Rb for quantization axes along the (a) z axis and (b) x axis when the laser is linearly polarized at an angle of 45° to the x axis.

previous studies of the intensity correlation in EIT [24–27], but our study differs in two ways.

The first difference is that the intensity correlation caused by the phase fluctuation of the incident laser is determined without combination of the orthogonal polarization components. The Hanle configuration is often used for preparing atomic coherence between Zeeman sublevels because it is possible to interact with the many degenerate Zeeman sublevels with a single laser. There is no relative phase noise among the optical transitions between the Zeeman sublevels in the Hanle configuration. In previous studies [24–26], there is the setup for combining the two polarization components before passing through the Rb atomic vapor cell, as shown in Fig. 1. In this setup, the phase fluctuation between two orthogonally polarized laser beams can be generated due to mechanical vibration and air flow. Therefore, the previous studies should be considered the additional phase fluctuation caused by the polarization combination process, as well as the phase fluctuation of the incident laser. However, in our experiment, a linearly polarized laser beam interacts with the EIT medium without the polarization combination process. After the beam has propagation through an EIT medium, we measure the intensity cross-correlation function between the selected two orthogonal polarization components of the phase fluctuation of the incident laser.

The second difference is that we investigated the dependence of the intensity correlations on the polarization basis. After the atom-light interaction, the polarization basis set for the intensity correlations of the linear or circular polarization was determined by changing the half-wave plate (HWP) or quarter-wave plate (QWP) (see the dashed gray box in Fig. 3). After the laser passed through the HWP or QWP, a second polarizer beam splitter (PBS) divided the beam into two orthogonal polarization components. To compare the intensity correlation of the EIT with the EIT spectra based on the polarization basis set, a flip mirror (FM) was inserted to allow observation of the EIT spectrum using the photodiode (PD). We measured the intensity fluctuations of each polarization component as a function of time using two avalanche photodiodes (APDs), and the intensity fluctuations δI_1 and δI_2 of the two APDs were estimated to be ± 50 mV. From the measured intensity fluctuations, the second-order cross-correlation function $g_{12}^{(2)}(\tau)$ of the orthogonally polarized components as a function of the time delay τ was calculated as

$$g_{12}^{(2)}(\tau) = \frac{\langle \delta I_1(t) \delta I_2(t+\tau) \rangle}{\sqrt{\langle \delta I_1(t)^2 \rangle \langle \delta I_2(t+\tau)^2 \rangle}}. \quad (1)$$

III. EXPERIMENTAL RESULTS AND DISCUSSION

The intensity fluctuations in the EIT between the two orthogonal polarization components are correlated because of the two-photon quantum coherence due to the interaction between the atoms and coherent optical field. In our experiment, the selection of the polarization basis after the Rb cell is a crucial factor that is related to the intensity fluctuations. Therefore we are interested in the role of the wave plate after the EIT medium.

To investigate how the intensity correlation depends on the polarization basis set, we measured $g_{12}^{(2)}(0)$ as a function of the

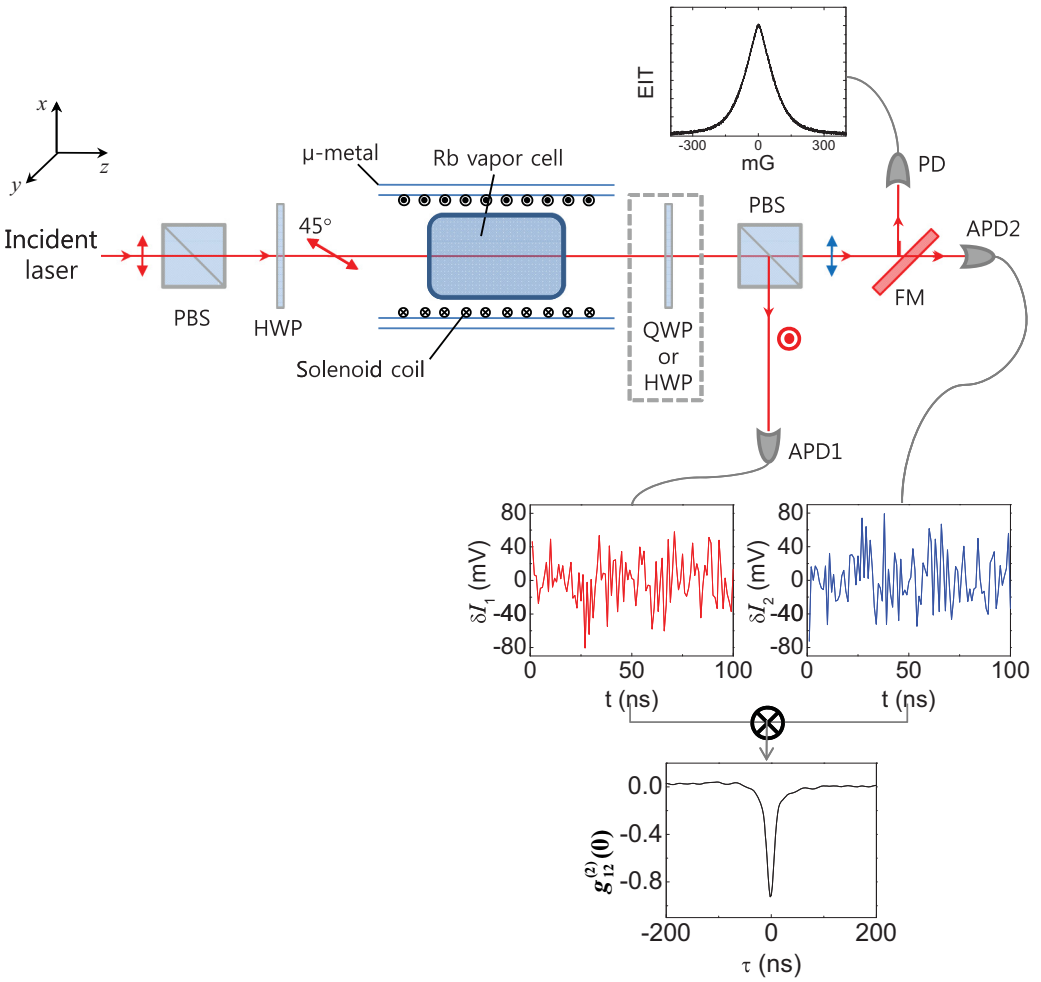

FIG. 3. (Color online) Schematic of our experimental setup for measuring the intensity correlation under EIT by selecting the orthogonal polarization basis after the atom-light interaction. PBS: polarizer beam splitter, PD: photodiode, APD: avalanche photodiode, QWP: quarter-wave plate, and HWP: half-wave plate.

applied B_l (parallel to the z axis in Fig. 3) for circular and linear polarization basis sets, as shown in Fig. 4. The power of the incident optical field was 2 mW, the laser beam diameter was approximately 2 mm, and the temperature of the Rb vapor cell was 100°C.

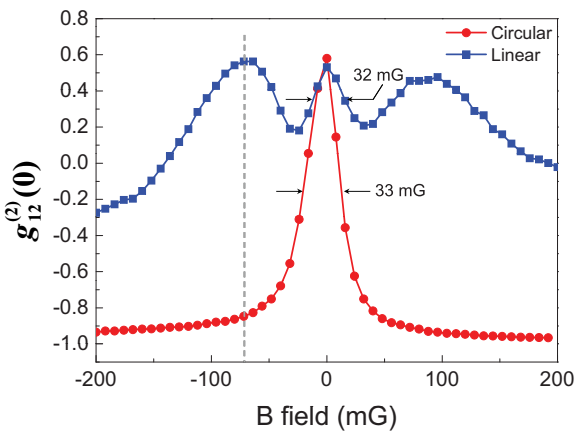

FIG. 4. (Color online) Measured $g_{12}^{(2)}(0)$ as a function of the applied longitudinal magnetic field B_l for circular (red circles) and linear (blue squares) polarization bases.

When we choose the circular polarization basis by using the QWP, we obtained $g_{12}^{(2)}(0)$ values for a B_l range of ± 200 mG, as shown by the red circles in Fig. 4. The values of $g_{12}^{(2)}(0)$ when the EIT system was on and off resonance were 0.6 (correlation) and -0.95 (anticorrelation), respectively, and the width of $g_{12}^{(2)}(0)$ was estimated to be 33 mG.

When the polarization basis was changed from circular to linear, we measured $g_{12}^{(2)}(0)$ as a function of B_l, shown by the blue squares in Fig. 4, and the shape of $g_{12}^{(2)}(0)$ is considerably different from that of the circular polarization basis. We found that $g_{12}^{(2)}(0)$ was greater than 0.2 (indicating correlation) in the range of -100 mG to $+100$ mG. The value of $g_{12}^{(2)}(0)$ on resonance was 0.6, and the width of $g_{12}^{(2)}(0)$ was estimated to be 32 mG, which is consistent with that of the circular polarization basis. However, the value of $g_{12}^{(2)}(0)$ near $B_l = \pm 70$ mG was 0.6 (correlation) for the linear polarization basis and -0.8 (anticorrelation) for the circular polarization basis, as indicated by the dashed gray line in Fig. 4. Interestingly, we could choose whether correlation or anticorrelation was measured by simply

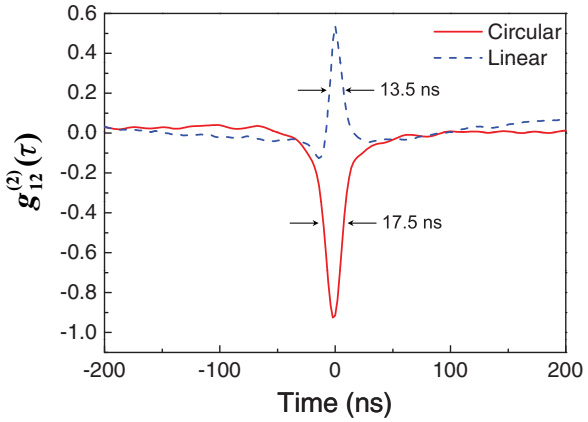

FIG. 5. (Color online) Measured $g_{12}^{(2)}(\tau)$ as a function of τ at $B_l = -72$ mG for the counter-rotating circular polarization basis (solid red curve) and perpendicular linear polarization basis (dashed blue curve).

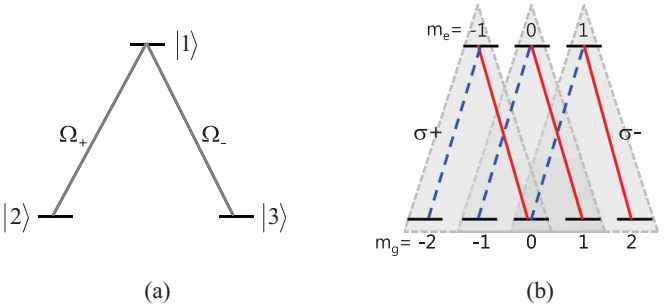

FIG. 6. (Color online) (a) Simple three-level atomic model consisting of one common excited state ($|1\rangle$) and two degenerate ground states ($|2\rangle$ and $|3\rangle$). (b) Eight-level atomic model consisting of three Λ-type configurations.

selecting the polarization basis after the atom-light interaction, as shown in Fig. 4.

Figure 5 shows $g_{12}^{(2)}(\tau)$ as a function of τ for $B_l = -72$ mG for the two polarization basis sets. We were able to observe an anticorrelation between the counter-rotating circularly polarized beams (solid red curve) and a correlation between the perpendicular linearly polarized beams (dashed blue curve). Under these two conditions, the linewidths of $g_{12}^{(2)}(\tau)$ were estimated to be 17.7 and 13.5 ns, respectively. From these results, although the laser field interacted with the atoms under the same conditions in both cases, the intensity correlation caused by the EIT in the presence of B_l depended on the polarization basis.

To understand these experimental results, we considered the simple three-level atomic model shown in Fig. 6(a). This model consists of one common excited state ($|1\rangle$) and two degenerate ground states ($|2\rangle$ and $|3\rangle$). Comparing the transitions of this three-level system with the transitions among the magnetic sublevels of the $5S_{1/2}\,(F_g = 2) \rightarrow 5P_{1/2}\,(F_e = 1)$ transition of ^{87}Rb in Fig. 2, we can consider the $|2\rangle \rightarrow |1\rangle$ and $|3\rangle \rightarrow |1\rangle$ transitions to represent the $\sigma^+\,(\Delta m = +1)$ and $\sigma^-\,(\Delta m = -1)$ transitions, respectively. To numerically solve the density-matrix equation in the three-level atomic system, we use the time-dependent Schrödinger equation in the density-matrix formalism:

$$\frac{\partial \hat{\rho}}{\partial t} = \frac{1}{i\hbar}[H_0 + H_{\rm int}, \hat{\rho}] + \frac{\partial \hat{\rho}_{sp}}{\partial t}, \tag{2}$$

where $\hat{\rho}$ is a density-matrix element, H_0 and $H_{\rm int}$ are the atomic and interaction Hamiltonians, respectively, and $\frac{\partial \hat{\rho}_{\rm sp}}{\partial t}$ is the relaxation term describing all the relaxation processes.

To interpret the intensity correlation and anticorrelation in the two polarization basis sets, we calculated $g_{12}^{(2)}(0)$ of the orthogonal polarization components based on the three-level atomic model. In the case of two counter-rotating circular polarizations (σ^+ and σ^- transitions), $g_{12}^{(2)}(0)$ in the three-level atomic model is

$$g_{12}^{(2)}(0) = \frac{{\rm Re}(\rho_{12}){\rm Re}(\rho_{13}) + {\rm Im}(\rho_{12}){\rm Im}(\rho_{13})}{\sqrt{[{\rm Re}(\rho_{12})^2 + {\rm Im}(\rho_{12})^2][{\rm Re}(\rho_{13})^2 + {\rm Im}(\rho_{13})^2]}}, \tag{3}$$

where ρ_{ij} is an atomic coherence term described by $\langle i|\hat{\rho}|j\rangle = \rho_{ij}$ for the $|i\rangle \rightarrow |j\rangle$ transition ($i \neq j$). Equation (3) is consistent with the value of $g_{12}^{(2)}(0)$ of the three-level Λ system [27].

However, in the case of orthogonal linear polarizations, the horizontal (H-pol) and vertical (V-pol) polarizations are considered to be equivalent to $\frac{\Omega_+ + i\Omega_-}{\sqrt{2}}$ and $\frac{\Omega_+ - i\Omega_-}{\sqrt{2}}$, respectively. The correlation between H-pol and V-pol depends on not only the absorption but also the polarization rotation. When the polarization rotation effect is also considered, Eq. (3) can be rewritten as

$$g_{12}^{(2)}(0) = \frac{(\bar{R}^2 - \Delta R^2 + \bar{I}^2 - \Delta I^2)}{\sqrt{[(\bar{R} + \Delta I)^2 + (\Delta R + \bar{I})^2][(\bar{R} - \Delta I)^2 + (\Delta R - \bar{I})^2]}}, \tag{4}$$

where $\bar{R} = {\rm Re}(\rho_{12}) + \kappa {\rm Re}(\rho_{13})$, $\Delta R = {\rm Re}(\rho_{12}) - \kappa {\rm Re}(\rho_{13})$, $\bar{I} = {\rm Im}(\rho_{12}) + \kappa {\rm Im}(\rho_{13})$, and $\Delta I = {\rm Im}(\rho_{12}) - \kappa {\rm Im}(\rho_{13})$. Here, κ describes the relative transition probability of the $|1\rangle \rightarrow |3\rangle$ transition to the $|1\rangle \rightarrow |2\rangle$ transition.

After numerically calculating the atomic coherence terms ρ_{ij} from the density-matrix equation of Eq. (2), we can numerically calculate $g_{12}^{(2)}(0)$ in the two types of polarization bases by applying Eqs. (3) and (4). To consider the intensity correlation effect of all magnetic sublevels, we calculated in an eight-level atomic model consisting of three Λ-type configurations, as shown in Fig. 6(b). Total intensity correlation is the average intensity correlation of three Λ-type configurations.

Considering the Doppler effect due to a moving atom in an atomic vapor cell, the $g_{12}^{(2)}(0)$ values as a function of B_l in the eight-level atomic model were calculated for the two cases of the circular and linear polarization bases, as shown in Fig. 7.

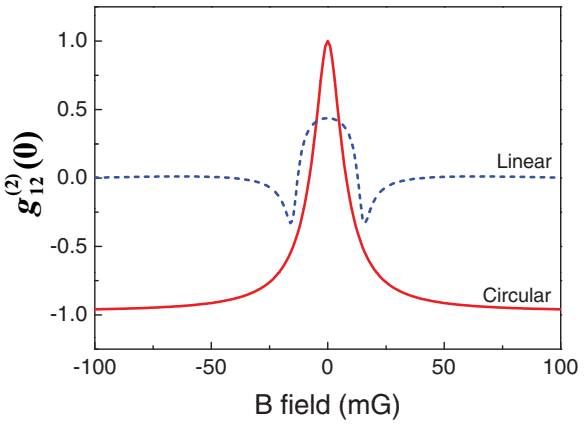

FIG. 7. (Color online) Calculated $g_{12}^{(2)}(0)$ as a function of B_l for circular (solid red curve) and linear (dashed blue curve) polarization bases.

The spontaneous decay rate Γ was $2\pi \times 6$ MHz. Also, the dephasing rate γ between the magnetic sublevels of the ground state was 150 kHz. In the case of the circular polarization basis, shown by the red solid curve of Fig. 7, the Rabi frequencies Ω_+ and Ω_- were all equal to Γ. The π transition is not considered in the case of the circular polarization basis. The blue dashed curve of Fig. 7 shows the calculated result of the intensity correlation for the linear polarization basis. A comparison with the experimental results in Fig. 4 reveals that the shapes of $g_{12}^{(2)}(0)$ as a function of B_l in both polarization bases are in good agreement with the measured $g_{12}^{(2)}(0)$ as a function of B_l. However, because our simple atomic model did not consider the atomic density and other hyperfine states, we were unable to account for the differences between the measured and calculated values of $g_{12}^{(2)}(0)$ at EIT resonance, but we can confirm that the degree of intensity correlation depends on the polarization basis selected after the atom-light interaction.

As reported in Ref. [27], the origin of the correlation and anticorrelation effects is the narrow transparency window (the imaginary part of the coherence term) and steep dispersion (the real part of the coherence term) around two-photon resonance. To understand the origin of the different features in the $g_{12}^{(2)}(0)$ as a function of B_l, we calculated the real and imaginary parts of the coherence terms in Eqs. (3) and (4). Figures 8(a) and 8(b) show the real and imaginary parts of the ρ_{12} and ρ_{13} coherence terms in Eq. (3) for two counter-rotating circular polarizations, respectively. In Fig. 8(a), we see that the signs of $\mathrm{Re}(\rho_{12})$ and $\mathrm{Re}(\rho_{13})$ are opposite, and hence, the sign of $\mathrm{Re}(\rho_{12})\mathrm{Re}(\rho_{13})$ in Eq. (3) will be negative. In contrast, Fig. 8(b) shows that $\mathrm{Im}(\rho_{12})$ and $\mathrm{Im}(\rho_{13})$ have the same sign, and so $\mathrm{Im}(\rho_{12})\mathrm{Im}(\rho_{13})$ in Eq. (3) will be positive. Therefore the real and imaginary parts of the coherence terms contribute to the anticorrelation and correlation, respectively. However, the sign of $g_{12}^{(2)}(0)$ at EIT resonance is positive because the magnitude of the imaginary part is larger than that of the real part. Away from EIT resonance, the sign of $g_{12}^{(2)}(0)$ is negative because the magnitude of the imaginary parts is larger than that of the real parts as the detuning from EIT resonance increases.

The real and imaginary parts of the coherence terms are related to the phase velocity and absorption of the transmitted light in the atomic medium. The intensity correlation between the two orthogonal polarization components is determined by the phase velocity and absorption of both components around two-photon resonance. The magnitude of each polarization component depends on the degree of absorption, and the polarization angle of the interacted light with the atomic medium depends on the phase difference between the two orthogonal polarization components. In the condition of EIT resonance, the phase difference is zero and the absorption signs of both polarization components are the same. So, the intensity correlation between the two orthogonal polarization components is positive at EIT resonance. On the other hand, in the case of off resonance, the phase difference between both polarization components increases and the polarization angle rotates. The relative magnitudes of both polarization components are anticorrelated because of separation of both components with the analyzer. Therefore the intensity correlation of both polarization components is negative at off resonance.

For the case of orthogonal linear polarizations, Fig. 9(a) shows the real terms $\bar{R}$ and ΔR in Eq. (4), while Fig. 9(b) shows the imaginary terms $\bar{I}$ and ΔI. Here, the relative transition probability κ was $1/6$, which corresponds to the Λ scheme with the $m_e = -1$ state in Fig. 6(b). In the case of the Λ scheme with the $m_e = 0$ state, ΔR and ΔI were both zero because $\kappa = 1$; the numerator and denominator in Eq. (4)

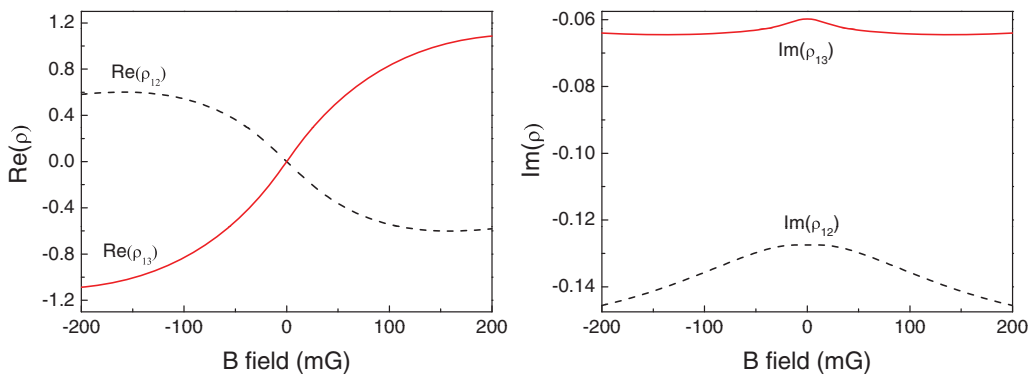

FIG. 8. (Color online) (a) Real and (b) imaginary parts of the ρ_{12} (dashed black curve) and ρ_{13} (solid red curve) coherence terms of the counter-rotating circular polarization basis.

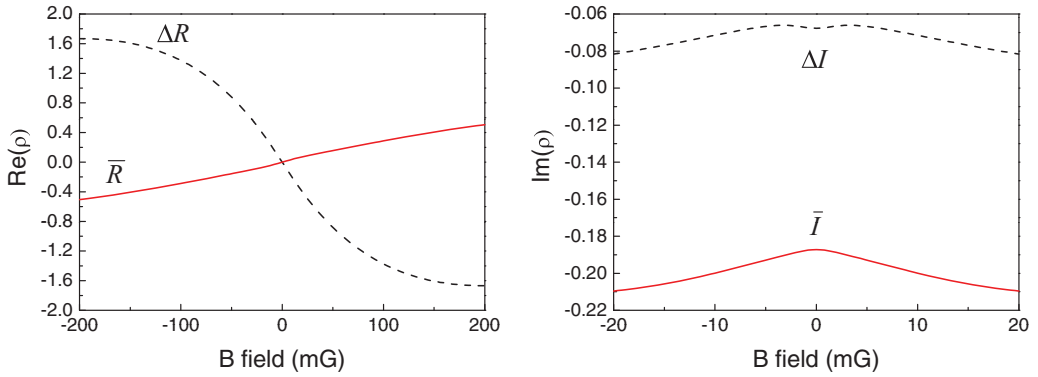

FIG. 9. (Color online) (a) $\bar{R}$ (solid red curve) and ΔR (dashed black curve) related to the real parts of the coherence terms and (b) $\bar{I}$ (solid red curve) and ΔI (dashed black curve) related to the imaginary parts of the coherence terms of the perpendicular linear polarization basis.

are then both $\bar{I}^2 + \bar{R}^2$, and so $g_{12}^{(2)}(0) = 1$ is independent of the magnetic field. The calculated result for the Λ scheme with the $m_e = +1$ state is the same as that with the $m_e = -1$ state (Fig. 9). Therefore the atomic coherence terms that contribute to the correlation for the linear polarization basis are completely different from those in the case of the circular polarization basis. From the calculated results, we were able to identify the origin of the different features in $g_{12}^{(2)}(0)$ as a function of B_l for the circular and linear polarization bases. After the atom-light interaction, the measurement basis for the intensity correlation determines whether there is correlation or anticorrelation between the two polarization components in the EIT medium.

IV. CONCLUSION

We have experimentally and theoretically investigated the variation in the intensity correlation and anticorrelation in an EIT system according to the polarization basis set chosen to split the beam after the atom-light interaction. The intensity correlation between the two polarization components was demonstrated in the Hanle configuration for the $5S_{1/2}\,(F = 2) \rightarrow 5P_{1/2}\,(F' = 1)$ transition of ^{87}Rb atoms. When the incident laser beam that was linearly polarized at an angle of 45° propagated through the Rb atomic vapor cell in the presence of a magnetic field, we were able to measure the $g_{12}^{(2)}(0)$ as a function of the applied B_l for both circular and linear polarization basis sets. We found that the shape of $g_{12}^{(2)}(0)$ in the linear polarization basis was completely different from that in the circular polarization basis. From the experimental results, we have confirmed that the intensity correlation under EIT depends on the polarization basis used for obtaining the orthogonal polarization components after the atom-light interaction. To understand the intensity correlation and anticorrelation in the two polarization bases, the $g_{12}^{(2)}(0)$ values were numerically calculated using an eight-level atomic model consisting of three Λ-type configurations. The shapes of the calculated $g_{12}^{(2)}(0)$ in both polarization basis sets were in good agreement with the measured $g_{12}^{(2)}(0)$. The $g_{12}^{(2)}(0)$ as a function of B_l for the circular and linear polarization bases differ as a result of the differences between the real and imaginary parts of the atomic coherence terms in the circular and linear polarization basis sets. We believe that our results will assist in understanding the quantum properties of atomic coherence.

ACKNOWLEDGMENTS

This research was supported by the Basic Science Research Program through the change to National Research Foundation of Korea (NRF) (Korea), funded by the Ministry of Education, Science, and Technology (Korea), 2012R1A2A1A01006579.

[1] K. J. Boller, A. Imamoglu, and S. E. Harris, Phys. Rev. Lett. **66**, 2593 (1991).
[2] M. Fleischhauer, A. Imamoglu, and J. P. Marangos, Rev. Mod. Phys. **77**, 633 (2005).
[3] J. Gea-Banacloche, Y.-q. Li, S.-z. Jin, and M. Xiao, Phys. Rev. A **51**, 576 (1995).
[4] Y. Wu and X. Yang, Phys. Rev. A **71**, 053806 (2005).
[5] M. D. Eisaman, A. André, F. Massou, M. Fleischhauer, A. S. Zibrov, and M. D. Lukin, Nature (London) **438**, 837 (2005).
[6] A. K. Mohapatra, T. R. Jackson, and C. S. Adams, Phys. Rev. Lett. **98**, 113003 (2007).
[7] T. Hong, C. Cramer, W. Nagourney, and E. N. Fortson, Phys. Rev. Lett. **94**, 050801 (2005).
[8] T. Zanon-Willette, A. D. Ludlow, S. Blatt, M. M. Boyd, E. Arimondo, and J. Ye, Phys. Rev. Lett. **97**, 233001 (2006).
[9] A. I. Lvovsky, B. C. Sanders, and W. Tittel, Nature Photon. **3**, 706 (2009).
[10] M. Fleischhauer and M. D. Lukin, Phys. Rev. Lett. **84**, 5094 (2000).
[11] A. Sinatra, Phys. Rev. Lett. **97**, 253601 (2006).
[12] J. Appel, E. Figueroa, D. Korystov, M. Lobino, and A. I. Lvovsky, Phys. Rev. Lett. **100**, 093602 (2008).

[13] E. Figueroa, M. Lobino, D. Korystov, J. Appel, and A. I. Lvovsky, New J. Phys. **11**, 013044 (2009).
[14] A. S. Zibrov, M. D. Lukin, and M. O. Scully, Phys. Rev. Lett. **83**, 4049 (1999).
[15] M. D. Lukin and A. Imamoglu, Nature (London) **413**, 273 (2001).
[16] A. Kuzmich, W. P. Bowen, A. D. Boozer, A. Boca, C. W. Chou, L.-M. Duan, and H. J. Kimble, Nature (London) **423**, 731 (2003).
[17] V. Balić, D. A. Braje, P. Kolchin, G. Y. Yin, and S. E. Harris, Phys. Rev. Lett. **94**, 183601 (2005).
[18] S. Du, P. Kolchin, C. Belthangady, G. Y. Yin, and S. E. Harris, Phys. Rev. Lett. **100**, 183603 (2008).
[19] P. Kolchin, C. Belthangady, S. Du, G. Y. Yin, and S. E. Harris, Phys. Rev. Lett. **101**, 103601 (2008).
[20] V. Boyer, A. M. Marino, R. C. Pooser, and P. D. Lett, Science **321**, 544 (2008).
[21] A. M. Marino, R. C. Pooser, V. Boyer, and P. D. Lett, Nature (London) **457**, 859 (2009).
[22] C. L. Garrido Alzar, L. S. Cruz, J. G. Aguirre Gómez, M. França Santos, and P. Nussenzveig, Europhys. Lett. **61**, 485 (2003).
[23] L. S. Cruz, D. Felinto, J. G. A. Gomez, M. Martinelli, P. Valente, A. Lezama, and P. Nussenzveig, Eur. Phys. J. D **41**, 531 (2007).
[24] V. A. Sautenkov, Y. V. Rostovtsev, and M. O. Scully, Phys. Rev. A **72**, 065801 (2005).
[25] T. S. Varzhapetyan, H. Li, G. O. Ariunbold, V. A. Sautenkov, Y. V. Rostovtsev, and M. O. Scully, Opt. Commun. **282**, 39 (2009).
[26] G. O. Ariunbold, Y. V. Rostovtsev, V. A. Sautenkov, and M. O. Scully, J. Mod. Opt. **57**, 1417 (2010).
[27] D. Felinto, L. S. Cruz, R. A. de Oliveira, H. M. Florez, M. H. G. de Miranda, P. Nussenzveig, M. Martinelli, and J. W. R. Tabosa, Opt. Express **21**, 1512 (2013).